

Elastic, Piezoelectric and Dielectric Properties of PIN-PMN-PT Crystals Grown by Bridgman Method

Jun Luo and Wesley Hackenberger
 TRS Technologies, Inc
 State College, PA, USA
 Email: jun@trstechnologies.com

Shujun Zhang and Tom R. Shrout
 Material Research Lab, Penn State,
 State College, PA, USA
 Email: soz1@psu.edu

Abstract — PIN-PMN-PT ($\text{Pb}(\text{In}_{1/2}\text{Nb}_{1/2})\text{O}_3\text{-Pb}(\text{Mg}_{1/3}\text{Nb}_{2/3})\text{O}_3\text{-PbTiO}_3$) single crystals with 26%-59% PIN were successfully grown by Bridgman technique. Elastic, dielectric and piezoelectric properties of ternary PIN-PMN-PT crystals were studied in comparison with PMN-PT ($\text{Pb}(\text{Mg}_{1/3}\text{Nb}_{2/3})\text{O}_3\text{-PbTiO}_3$) crystals. It was demonstrated that PIN-PMN-PT crystals possess as excellent piezoelectric properties as PMN-PT crystals, but can be operated at elevated temperature and AC electric field without the depoling issue. T_{RT} of PIN-PMN-PT crystals with 26%-36% PIN were roughly in the range of 115 -135°C, 30-40°C higher than that of PMN-PT crystals; meanwhile, E_{C} were on the order of 4.5-5.6kV/cm, two to three times higher than that of PMN-PT crystals. A full set of measured or derived elastic, piezoelectric and dielectric properties of PIN-PMN-PT crystals are present in this paper.

Keywords-PIN-PMN-PT, single crystal, elastic property, piezoelectric property and dielectric property

I. INTRODUCTION

Single crystal relaxor ferroelectrics, $\text{Pb}(\text{Mg}_{1/3}\text{Nb}_{2/3})_{1-x}\text{Ti}_x\text{O}_3$ (PMN-PT), have shown great promise for broad bandwidth compact transducers[1-3]. In comparison with traditional sensor array materials, the compliance of PMN-PT is 4.5 times that of PZT-4. This allows the element size for a given resonance frequency to be reduced. PMN-PT has a piezoelectric d_{33} coefficient of 6.5 times that of PZT-4, which will allow the shorter element to maintain acoustic intensity. Lastly, the electromechanical coupling coefficient, k_{33} , for PMN-PT is greater than 90 percent compared to 70 percent for PZT-4. The large coupling coefficient provides a much larger operating bandwidth

Several key issues need to be addressed to continue development of single crystal technology. PMN-PT crystals have a lower phase-transition temperature (80-95°C) and a strong temperature dependence of the dielectric constant, which not only limit the maximum usage temperature, but also negatively affect the transducer impedance matching with the power delivery system. Meanwhile, PMN-PT possesses very low coercive field (1.8-2.5kV/cm), so DC bias may be required to prevent depoling under AC field with comprises on the performance and cost.

This research is sponsored by Office of Naval Research through SBIR programs

In recent years, more and more efforts have been made on investigating new single crystal piezoelectrics that can operate at higher temperature and higher electric field than current state-of-the-art PMN-PT single crystals. It has been demonstrated that ternary PIN-PMN-PT ($\text{Pb}(\text{In}_{1/2}\text{Nb}_{1/2})\text{O}_3\text{-Pb}(\text{Mg}_{1/3}\text{Nb}_{2/3})\text{O}_3\text{-PbTiO}_3$) crystals can potentially be such a candidate[4-6]. In this work, the dielectric, piezoelectric and elastic properties of PIN-PMN-PT crystals were studied in comparison with the binary PMN-PT counterpart.

II. EXPERIMENTAL

A. Bridgman growth of PIN-PMN-PT single crystals

Ternary PIN-PMN-PT single crystals were grown by the self-seeded and seeded Bridgman technique. The starting composition was selected as PIN-PMN-PT with 26-59% PIN and 28-32%PT. However, for the compositions with PIN content higher than 36%, the melt became less stable and pyrochlore phase formed during solidification. In Bridgman growth process, the cylindrical Pt crucibles charged with PIN-PMN-PT starting materials were placed in a two-zone furnace. By setting temperature of the upper-zone 80-120°C higher than the melting point and 300-500°C higher than that in the lower-zone, an axial temperature gradient of 30~50 °C/cm formed between two zones. After the charge was melted in Pt crucible in the upper-zone, the crucible was lowered down slowly through the temperature gradient to accomplish the unidirectional crystallization process. The PIN-PMN-PT single crystals with diameter up to 50mm were grown along both <111> and <110> orientations. An obtained crystal boule with 50 mm in diameter and 100 mm in length is shown in Fig. 1

B. Elastic, piezoelectric and dielectric property measurement

As reported for PMNT crystals, the composition along the growth direction varies due to the segregation of titanium in PIN-PMN-PT crystals, with lower PT content at the bottom part of the crystal and the crystal near the top of the boule was found to be in tetragonal phase. All the samples for characterization in this work belong to the rhombohedral



Figure 1. A photo of PIN0MN-PT crystal with 50mm diameter

phase with the composition close to MPB (26-36%PIN and 28-32%PT). The full set of material constants was determined using the resonance method and five types of Z-cut samples were prepared according to IEEE standards [7-12]. All the samples were oriented along their crystallographic directions [001] and [110] using real-time Laue and sputtered with gold on the parallel [001] faces. The samples were poled at 20kV/cm at room temperature. The Curie temperature (T_C) and rhombohedral-to-tetragonal phase transition temperatures (T_{RT}) were determined from the dielectric temperature dependence using a multifrequency LCR meter (HP4284A), connected to a computer controlled temperature chamber. High field polarization and strain measurements at room temperature were performed on [001] oriented plate samples using a modified Sawyer-Tower circuit and linear variable differential transducer (LVDT) driven by a lock-in amplifier. The resonance and anti-resonance frequencies were obtained by an HP 4194A Impedance- phase gain analyzer under low field.

III. RESULTS AND DISCUSSIONS

A. Comparison of T_{RT} and T_C between PIN-PMN-PT and PMN-PT crystals

Fig. 2 shows the similar tendency of T_C and T_{RT} as a function of location in a PIN-PMN-PT and a PMN-PT crystal boule respectively, which was mainly impacted by the similar Ti segregation along the boules. However, PIN-PMN-PT possessed consistently higher T_C and T_{RT} at the same location of each boule, which was obviously corresponded to In substitution and its nearly even distribution along the boule. An average T_{RT} increase of 35°C to 40°C was observed in this PIN-PMN-PT boule in comparison with the PMN-PT boule, which extended the usage temperature to 120°C - 135°C. In this PIN-PMN-PT boule, the T_C and T_{RT} were found to be 230°C and 90°C, respectively at top of the crystal boule, corresponding to higher PT content in the crystals. The piezoelectric coefficient was found to be 1800-2200pC/N. Samples at the bottom part of the crystal boule, with lower PT concentration, exhibited lower T_C of ~180°C and higher T_{RT} of ~135°C, with piezoelectric coefficients on the order of 1000-1200pC/N.

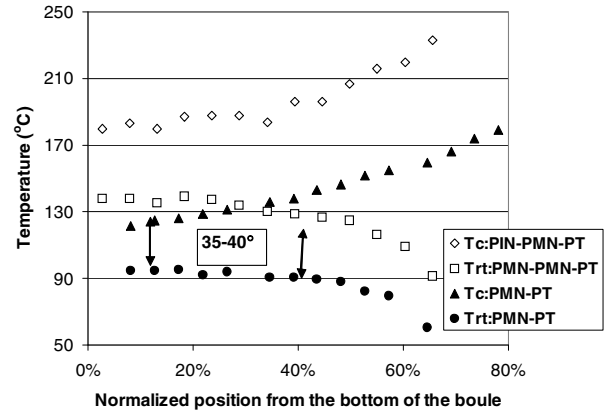


Figure 2. T_C and T_{RT} as a function of location in a PIN-PMN-PT and a PMN-PT crystal boule

B. Comparison of dielectric constant between PIN-PMN-PT and PMN-PT crystals

Fig. 3 shows the dielectric permittivity as a function of temperature for a rhombohedral PIN-PMN-PT compared to PMN-29PT. The room temperature dielectric permittivity was found to be 4000-4500, lower than binary PMN-29PT crystal (~5400). The dielectric permittivity variation for PIN-PMN-PT in the range of room temperature to 100°C was found to be on the order of ~50/°C or ~1.1%/°C, much lower when compared to PMNT crystal (~220/°C or ~4%/°C), exhibiting a much flatter and more stable dielectric behavior. The dielectric loss for PIN-PMN-PT crystals were found less than 1% at room temperature, exhibiting similar trend as dielectric permittivity, with peak values located at the phase transition temperature.

C. Comparison of k_{33} and d_{33} between PIN-PMN-PT and PMN-PT crystals

Fig. 4 shows the variation of electromechanical coupling k_{33} and piezoelectric coefficient d_{33} as a function of

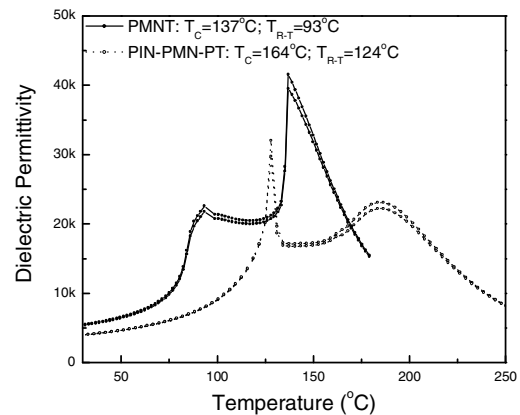


Figure 3. The dielectric permittivity as a function of temperature for a rhombohedral PIN-PMN-PT compared to PMN-29PT

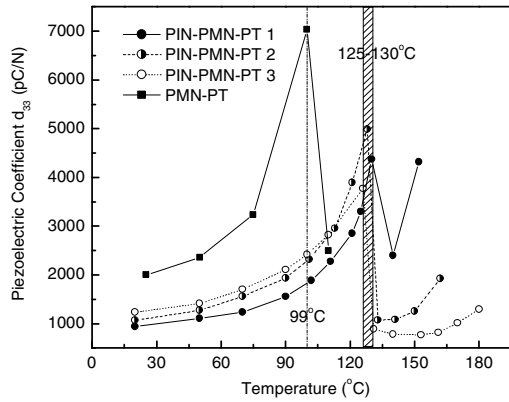
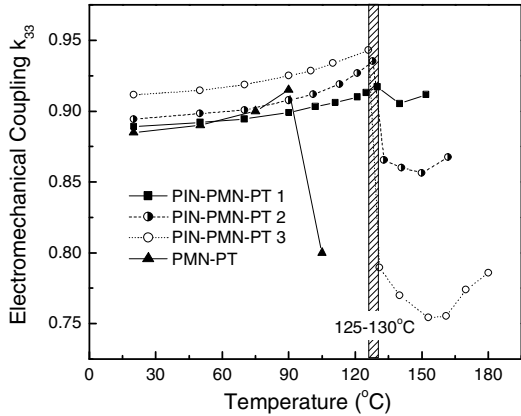


Figure 4. The variation of electromechanical coupling k_{33} and piezoelectric coefficient d_{33} as a function of temperature for PIN-PMN-PT crystals compared to PMNT

temperature for PIN-PMN-PT crystals, compared to PMNT. [001] oriented longitudinal rods were measured in the temperature range of 20-180°C. It was observed that the electromechanical coupling factor maintained similar values with increasing temperature, decreasing sharply above the phase transition temperature ($\sim 125^\circ\text{C}$ for PIN-PMN-PT), due to the partial depolarization of the crystals in the tetragonal phase. The piezoelectric coefficients were found to increase with increasing temperature and reach a maxima at the phase transition temperature, whereupon they decreasing significantly. It is obvious that, not only PIN-PMN-PT had much higher phase transition temperature than PMN-PT, but also the temperature dependences of k_{33} and d_{33} were much less than those of PMN-PT crystals.

D. Polarization and strain measurement of PIN-PMN-PT

Fig. 5 shows the polarization and butterfly strain behaviors measured for three PIN-PMN-PT samples orientated along the [001] direction. It was found that the coercive field of PIN-PMN-PT crystal was on the order of 4.5-5.6kV/cm for slightly different PT content, which was increased by 2-3 times compared to PMN-29PT crystals.

Due to the low coercive field, for PMN-PT crystal transducers driven by AC field, DC bias were always desired to prevent the material from depoling. The elevated E_C of PIN-PMN-PT crystals may eliminate DC bias or at least lower down DC bias field significantly in such applications. In the unipolar and bipolar strain measurement, PIN-PMN-PT crystals showed linear strain behavior with no hysteresis before the field induced phase transition happened. The observed DC field to induce phase transition in PIN-PMN-PT crystals was much higher than that in PMN-PT crystals, which means that PIN-PMN-PT can be driven much harder than PMN-PT under DC field without inducing any phase-transition related non-linearity. It was observed that the phase transition only happened when electric field was beyond 50kV/cm for most of PIN-PMN-PT crystal samples; on the contrary, PMN-PT crystal usually experienced phase transition under the field of 15 to 30kV/cm.

E. Full set of elastic, piezoelectric and dielectric properties of PIN-PMN-PT crystals

Table I through Table III list the full set of elastic constants, piezoelectric coefficients, electromechanical

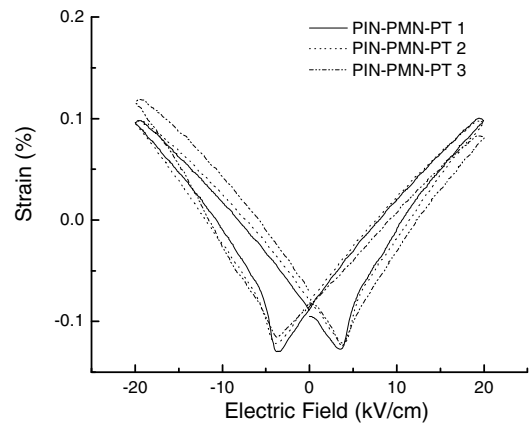
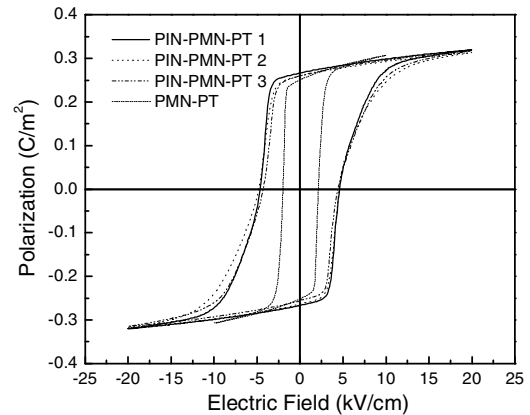


Figure 5. The polarization and butterfly strain behaviors measured for three PIN-PMN-PT samples orientated along the [001] direction

coupling factors and dielectric permittivity for PIN-PMN-PT and compared to PMN-29PT. As can be seen in Table I, the elastic compliance and stiffness constants of measured PIN-PMN-PT crystals and PMN-29PT crystals are quite similar. From Table II, it was found that the electromechanical couplings, k_{33} , k_{31} and $k_{31}(45^\circ)$ of them are very similar as well, while the piezoelectric coefficients, d_{33} and e_{33} , of the measured PIN-PMN-PT crystals are slightly lower than those of PMN-29PT crystal, which might be directly related to the relatively low dielectric constants, ϵ_{33}^T and ϵ_{33}^S .

TABLE I. MEASURED AND DERIVED ELASTIC COMPLIANCE CONSTANTS, $S_{ij}(10^{-12} \text{ m}^2/\text{N})$, AND ELASTIC STIFFNESS CONSTANTS, $c_{ij}(10^{10} \text{ N/m}^2)$, FOR PIN-PMN-PT CRYSTALS, COMPARED TO PMNT29.

Material	S_{11}^E	S_{12}^E	S_{13}^E	S_{33}^E	S_{44}^E	S_{66}^E
PIN-PMN-PT	49.0	-20.0	-26.5	57.3	15.2	39.4
PMNT29	52.1	-24.6	-26.4	59.9	16.0	28.3
Material	S_{11}^D	S_{12}^D	S_{13}^D	S_{33}^D	S_{44}^D	S_{66}^D
PIN-PMN-PT	38.2	-30.8	-4.0	10.3	14.3	39.4
PMNT29	41.8	-34.8	-3.9	10.3	14.0	28.3
Material	C_{11}^E	C_{12}^E	C_{13}^E	C_{33}^E	C_{44}^E	C_{66}^E
PIN-PMN-PT	11.9	10.5	10.4	11.4	6.6	2.5
PMNT29	12.4	11.1	10.4	10.8	6.3	3.5
Material	C_{11}^D	C_{12}^D	C_{13}^D	C_{33}^D	C_{44}^D	C_{66}^D
PIN-PMN-PT	12.3	10.9	9.0	16.7	7.0	2.5
PMNT29	12.6	11.3	9.3	16.8	7.1	3.5

TABLE II. PIEZOELECTRIC COEFFICIENTS, d_{ij} (pC/N), e_{ij} (C/m²), g_{ij} (10⁻³ Vm/N), h_{ij} (10⁶ V/m), AND ELECTROMECHANICAL COUPLING FACTORS, k_{ij} , FOR PIN-PMN-PT CRYSTALS, COMPARED TO PMNT29.

Material	d_{33}	d_{31}	d_{15}	e_{33}	e_{31}	e_{15}
PIN-PMN-PT	1320	-634	105	18.6	-4.8	6.9
PMNT29	1540	-699	164	22.3	-3.9	10.3
Material	g_{33}	g_{31}	g_{15}	h_{33}	h_{31}	h_{15}
PIN-PMN-PT	35.6	-17.0	8.8	28.9	-7.4	6.5
PMNT29	32.2	-14.6	11.9	27.7	-4.8	8.7
Material	k_{33}	k_{31}	k_{15}	k_t	$k_{31}(45^\circ)$	
PIN-PMN-PT	0.91	0.47	0.25	0.57	0.80	
PMNT29	0.91	0.44	0.35	0.60	0.81	

TABLE III. DIELECTRIC CONSTANTS, ϵ_{ij} (ϵ_0), AND DIELECTRIC IMPERMEABILITY CONSTANTS, β (10⁻⁴/ ϵ_0), FOR PIN-PMN-PT CRYSTALS, COMPARED TO PMNT29.

Material	ϵ_{33}^T	ϵ_{11}^T	ϵ_{33}^S	ϵ_{11}^S
PIN-PMN-PT	4200	1335	729	1200
PMNT29	5400	1560	910	1340
Material	β_{33}^T	β_{11}^T	β_{33}^S	β_{11}^S
PIN-PMN-PT	2.38	7.49	13.72	8.33
PMNT29	1.85	6.41	10.99	7.46

IV. CONCLUSIONS

Large size (50mm in diameter) PIN-PMN-PT crystals were grown directly from the melt using the Bridgman

technique. The piezoelectric properties of rhombohedral PIN-PMN-PT crystals are comparable to binary PMNT crystals. Of particular interest, the rhombohedral-to-tetragonal phase transition temperatures and the coercive field observed were on the order of 115-135°C and 4.5~5.6kV/cm respectively. In summary, due to the higher Curie temperature, PIN-PMN-PT crystals were found to possess higher coercive field, more stable dielectric and piezoelectric properties and much broader usage temperature range, when compared to PMNT crystals, make the ternary crystals promising candidates for wider range of potential transducer applications.

ACKNOWLEDGMENT

This work was supported by the ONR under No. N00014-07-C-0858 and NIH under No. P41-RR11795.

REFERENCES

- [1] S. E. Park and T. R. Shrout, J. Appl. Phys. **82**, 1804 (1997).
- [2] S. J. Zhang, J. Luo, R. Xia, P. W. Rehrig, C. A. Randall and T. R. Shrout, Solid State Commun., **137**, 16 (2006).
- [3] D. Damjanovic, M. Budimir, M. Davis and N. Setter, J. Mat. Sci. **41**, 65 (2006).
- [4] Y. P. Guo, H. S. Luo, T. He and Z. W. Yin, Solid State Commun., **123**, 417 (2002).
- [5] G. S. Xu, K. Chen, D. F. Yang and J. B. Li, Appl. Phys. Lett., **90**, 032901 (2007).
- [6] J. Tian, P. D. Han, X. L. Huang and H. X. Pan, Appl. Phys. Lett., **91**, 222903 (2007).
- [7] S. J. Zhang, C. A. Randall and T. R. Shrout, J. Appl. Phys., **95**, 4291 (2004).
- [8] S. J. Zhang, S. M. Lee, D. H. Kim, H. Y. Lee and T. R. Shrout, J. Appl. Phys. **102**, 114103 (2007).
- [9] *IEEE Standard on Piezoelectricity* (ANSI/IEEE Standard, NY, 1987-176).
- [10] W. W. Cao, Handbook of Adv. Dielect. Piezoelect. and Ferroelect. Mater: Synthesis Characterization and Applications, edited by Z. G. Ye, (Woodhead Publishing Limited, Cambridge, 2008), pp.235.
- [11] S. J. Zhang, S. M. Lee, D. H. Kim, H. Y. Lee and T. R. Shrout, J. Am. Ceram. Soc., **91**, 683 (2008).
- [12] X. C. Geng, T. A. Ritter and S. E. Park, in *IEEE Ultrason. Symposium* (IEEE 1998) p.571.